International Journal of Horticultural Science and Technology
Journal homepage: http://ijhst.ut.ac.ir

A Gold Nanoparticle-Based Colorimetric Probe for Detection of Gibberellic Acid Exuded by *Ralstonia solanacearum* Pathogen in Tomato (*Solanum lycopersicum* L.)

Ivy Lynn Aoko[1]*, Dezzline Ondigo[2], Agnes Mumo Kavoo[1], Cornelius Wainaina[1], and Leonard Kiirika[1]

1. Department of Horticulture and Food Security, Jomo Kenyatta University of Agriculture and Technology, P.O. Box 62000–00200 Nairobi, Kenya
2. Department of Physical Sciences, Karatina University, P.O. Box 1957-10101 Karatina, Kenya

ARTICLE INFO

Article history:

Received: 16 October 2020
Received in revised form: 3 January 2021
Accepted: 27 January 2021

Article type:

Research paper

Keywords:

Bacterial wilt,
Biosensor,
AuNPs,
Tomato.

ABSTRACT

We report a simple colorimetric probe based on gold nanoparticles (AuNPs) for detecting *Ralstonia solanacearum*. The AuNPs were synthesized through reduction with citrate ion and characterized by ultraviolet-visible spectroscopy (UV-vis), scanning electron microscopy (SEM), and transmission electron microscopy (TEM). The freshly synthesized AuNPs were brick red due to an intense surface plasmon absorption band at 520 nm. Upon interaction with synthetic gibberellic acid (GA_3), a bathochromic shift occurred in the surface plasmon resonance (SPR) peak of AuNPs to higher wavelengths. The 'eye-ball' limit of detection was 0.2 ppm. This shift was accompanied by a change in the color of the AuNPs from brick red to purple. Soil samples were collected from the rhizosphere of tomato plants, exhibiting bacterial wilt symptoms and pure cultures of *Ralstonia solanacearum* isolated using a modified Kelman's TZC medium. Gibberellins (GA) were extracted from the culture of *R. solanacearum* using ethyl acetate and characterized using fourier transform infrared spectroscopy (FT-IR). AuNP solution aggregation was induced by GA-mediated *R. solanacearum.* A color change from brick red to purple was also observed. The results illustrated the use of both SPR wavelength-shift sensing and visual color change to detect molecules of biological relevance.

Introduction

Ralstonia solanacearum is a soil-borne pathogen that infects the plant host in favorable conditions by attacking to the plant roots through physical wounds, and infection of the cortex and colonization in the xylem (Afroz et al., 2013). During the host infection process, the pathogen multiplies and produces exopolysaccharides within the water-conducting system; thus, the host wilts, collapses and dies due to clogging (Khan, 2014). The pathogen can enter into a viable but not culturable state under unfavorable conditions and, as such, can build up inoculum potential and remain attached to a carrier for

* Corresponding Author, Email: lynnaoko@gmail.com

an extended period (Ponce et al., 2013; Slistan-Grijalva et al., 2005). *Ralstonia solanacearum* is highly versatile, making it difficult to control after host infection, hence early detection and prevention is an important aspect in disease management (Mirkin et al., 1996).

Detection of bacterial wilt incidence in tropical developing countries is essential since the pathogen is endemic (Li et al., 2008). A clear understanding of the interaction process between the host and the pathogen is essential in devising detection tools. During the microbe-host interaction *in vitro*, bacteria within the soil rhizosphere produce hormones such as auxins, gibberellins (GA), cytokinins, ethylene, and abscisic acid (Katznelson & Cole, 1965). Previous studies have revealed that bacteria inhabiting various plants' rhizosphere are likely to synthesize and release gibberellins (GAs) as secondary metabolites (Bertolini & Olmos, 2004; Primo et al., 2015). GAs and GA-like substances are a class of physiologically important phytohormones produced and transferred in plant cells as metabolites during plant–*Ralstonia* interaction (Jiang et al., 2017). They play a role as a signaling factor towards the host plant (Karuku et al., 2017). Gold nanoparticles (AuNPs) can bind with a wide range of organic molecules (Jing et al., 2019), so they can be useful in devising tools to detect specific target molecules produced by pathogens. Crop losses can be reduced by developing the specific treatments to control the diseases if the causing agents are accurately diagnosed and identified before spreading (Tyagi et al., 2016a). Despite this knowledge, bacterial wilt remains a major limiting factor to tomato production due to lack of detection methods for the disease.

Conventional methods for identifying bacterial wilt include microscopic and cultural techniques, which are time-consuming and require complicated sample preparation steps and a high cost of instruments (Verma et al., 2014). Besides, they are often prone to errors because of probable losses during sample collection, transportation, and pre-treatment (Hennessy et al., 1996) before the actual analysis. Therefore, developing simple, selective and easy-to-use methods by non-skilled farmers is required. Colorimetric probes can overcome these limitations since signaling the targeted event can be visualized by "naked eyes" (Mansfield et al., 2012). Colorimetric probes are materials that bind selectively with the analyte to give a distinctive color change. Many materials are used in the fabrication of colorimetric probes including organic dyes, synthetic ligands, nanomaterials (i.e., TiO_2 NPs, SiO_2 nanoparticles; quantum dots (e.g., CdSe and CdTe); AuNPs, AgNPs, CuNPs (Park & Shumaker-parry, 2020). Metallic nanoparticles are particularly attractive for a color signal generation; they possess much higher extinction coefficients than organic dyes and synthetic ligands, allowing sensitive colorimetric detections with minimal material consumption (Bhalla et al., 2010). The metal nanoparticles based colorimetric assays do not utilize organic co-solvents, enzymatic reactions, light-sensitive dye molecules, lengthy protocols, or sophisticated instrumentation, therefore, overcoming some of the limitations posed by conventional methods. More importantly, metallic nanoparticles are known to display distance-dependent optical properties (Draz & Shafiee, 2018). Analyte induced dispersion or aggregation of nanoparticles resulting in a distinctive color change can be used as a sensing mechanism for detecting various biomolecules.

AuNPs are attractive materials for developing colorimetric probes due to their color, mainly based on the surface plasmon resonance, and they also display distant dependent optical properties (Kim et al., 2015; Stevens & Jaykus, 2014). For example, dispersed AuNPs are red, while aggregated ones are purple or blue (Jazayeri et al., 2018). Colorimetric probes using metal nanoparticles have been widely explored and successfully used in the sensitive detection of metal ions

(Murigi et al., 2014; Sciences et al., 2013). This study aimed at designing a simple colorimetric probe to detect the presence of GA-mediated *R. solanacearum* based on AuNPs aggregation, making detection of the bacterial wilt of tomato possible.

Materials and Methods

Materials and reagents

All A Gold Nanoparticle Fisher Scientific, UK and LobaChemiePvt Ltd. including Chloroauric acid (ACS reagent ≥ 49.0, Au basis $Haucl_4.H_20$, mw = 357.8018 g/mol), tri-Sodium citrate dehydrate ($C_6H_5Na_3O_7.2H_2O$, mw = 294.09 g/mol, 99%) and sodium chloride (NaCl, mw = 58.44 g/mol).

Instrumentation

The morphology, size, and shape of AuNPs were evaluated using a scanning electron microscope FEI XL30 Sirion FEG (Oxford Instruments Plc, Abingdon, United Kingdom) operated at an accelerating voltage of 30 kV. The system was equipped with an Energy Dispersive x-ray Spectrometer (EDS) system from EDAX, having a lithium doped silicon detector (Ngumbi et al., 2018). TEM micrographs were acquired on a Tecnai G2 Spirit (Thermo Fisher Scientific, Oregon USA) operated at 120 kV after suspending the pulp fibers in ultrapure water (18 MΩ.cm Barnstead Genpure UV-TOC, Thermo Fisher Scientific, Germany), and drop-casting on carbon films 300 mesh (Electron microscopy science, CF300-CU). The particle size distribution, zeta potential, and poly-dispersibility index were measured using a Bechman Coulter DelsaMax pro Dynamic light scattering analyzer (Indianapolis, United States). Electronic absorption spectra were recorded on a Shimadzu (Shimadzu Japan) UV/VIS 1800 spectrophotometer in a quartz cell (1 cm) in the region between 300-800 nm. Using Fourier transform infrared spectroscopy (FT-IR), FT-IR spectra were recorded using a Shimadzu 8400 Fourier Infrared spectrophotometer (Shimadzu, Japan). The samples were spotted on KBr discs and analyzed between the scanning range from 400 to 4000 cm^{-1} (Bottini et al.,2004; Kapoor, Soni, & Kaur, 2016; Selvarajan et al., 2020).

Synthesis of AuNPs

AuNPs were synthesized using the citrate reduction method, as described in the literature by Huang et al. (2015).

Optimization of reaction conditions during the synthesis of AuNPs

The pH stability, temperature, and reaction time during synthesizing AuNPs were studied by subjecting the AuNPs solutions to different pH conditions and measuring the absorbance spectra on UV/VIS. The pH was adjusted by either adding drops of 1N NaOH or 1N HCl until the desired pH was achieved. Varying temperature and reaction periods were also investigated. The UV/VIS spectra were analyzed by plotting graphs of absorbance against wavelength, and the appearance of absorption spectra was used to confirm the pH stability of the AuNPs (Huang et al., 2015).

Collection of soil samples and isolation of R. solanacearum

Soil samples were collected from the rhizosphere of tomato plants, exhibiting bacterial wilt symptoms in Kajiado, Kiambu, Bomet, and Kirinyaga counties in Kenya.

These counties are reported where are reported to experience huge crop losses due to the bacterial wilt soil-borne pathogen (Jongjinakool et al., 2014; Sarkar & Chaudhuri, 2016). The soil samples were collected in sterile polythene sampling bags and stored at 4 ˚C for further processing. *Ralstonia solanacearum* strains were isolated by suspending 10 g soil samples into 250 mL of conical flasks containing 90 mL of sterile distilled water. The suspension was thoroughly mixed by shaking on a rotary shaker for 10 min, to dislodge bacterial cells held within the soil colloids. The obtained bacterial cell

suspension was serially diluted (by a 10^{-3} dilution factor), and 10 µL and 20 µL plated on containing Nutrient agar (NA) amended with Kelman's Tetrazolium Chloride (TZC). The bacterial cultures were incubated at 28˚C for 24 h and *R. solanacearum* colonies were identified by their large and elevated size, fluidal nature, and color. Bacterial cell count was done using a standard plate count method and recorded as colony forming units (CFU)/ml of the sample.

Extraction of GAs

Ralstonia solanacearum colonies exhibiting virulent characteristics were selected and grown on Nutrient Broth (NB) medium on a rotary shaker at 28 ˚C for 48 h. A supernatant of bacterial cells was obtained by centrifugation and GA_3 extracted using ethyl acetate in a ratio of 1:3 according to the protocol by Sharma, Sharma, & Kaur, 2018.

Quantification of GAs using HPLC analysis

A reverse-phase HPLC was used for the quantification of GAs. The stationary phase consisted of LiChrospher on the RP-18 packed stainless-steel column (250 x 4 mm i.d.), and the chromatograms were recorded on an NT-based chemstation program. Acetonitrile and acidic water (60:40 v/v in 0.01 % H_3PO_4) were used as the mobile phase with a flow rate of 0.5 mL min^{-1}. The obtained extracts were filtered through 0.45 µm membrane filters. Synthetic GA_3 was used as a standard. Standard solutions of GA_3 were prepared by dissolving 50 mg of GA_3 in 10 mL acetonitrile. Working standards of 0.1-1.0 ppm were prepared by serial dilution and 20 µL of each standard concentration injected in HPLC set at a wavelength of 206 nm (Sharma et al., 2018). After standardization, 20 aliquots of real samples containing extracted GAs were injected under the same conditions. GAs extracted from the culture of a singular isolate of *R. solanacearum* (in triplicate) obtained from Juja subcounty, Kiambu county showed peaks similar to that of the standard GAs in HPLC analysis.

Sensitivity studies

The sensing mechanism of the AuNPs probe was initially carried out using synthetic GA_3 at varying concentrations (0.1-1.0 ppm). In a typical experiment, the GA solution was added to 1800 L of AuNPs solution (Godoy-reyes & Costero, 2019), and the resultant mixture was monitored for observable color change.

FT-IR Analysis of GA-mediated R. solanacearum

GAs were extracted and separated from the supernatant with ethyl acetate (Bhalla et al., 2010). The presence of GAs in the isolate was confirmed using Infra-Red Spectroscopy (FT-IR). The FT-IR spectra of extracted GA_3 were compared with the standard spectrum of GA_3.

Detection of GA-mediated R. solanacearum from Real Samples

Ralstonia solanacearum inoculum (previously isolated from soil samples) was prepared at varying levels (10^4 CFU/mL, 10^6 CFU/mL, and 10^8 CFU/mL). The prepared inoculum was added to the nanoparticle solution at a ratio of 1:1 (v/v), and changes in absorbance were monitored (Ngumbi et al., 2018) using a UV-visible spectrophotometer. Soil samples that had been previously collected from the rhizosphere of tomato plants exhibiting bacterial wilt were tested to determine the presence of *R. solanacearum*.

Results

Optimization of reaction conditions during synthesis of the AuNPs

During the AuNPs synthesis, we observed varying effects of different reaction conditions. The optimal pH conditions were determined between 6.5 and 11.5, while optimum temperature and reaction times ranged from 50-90 ˚C and 6-24 min, respectively.

Morphology and size of the synthesized AuNPs

The morphology of the freshly synthesized AuNPs was observed using a scanning electron microscope (SEM). The AuNPs were dispersed, as shown in SEM micrographs (Fig. 2A insert). The dispersed nature of the nanoparticles was further confirmed by the TEM micrographs (Fig. 2B insert). Differences in the size of NPs can be attributed to varying reaction conditions.

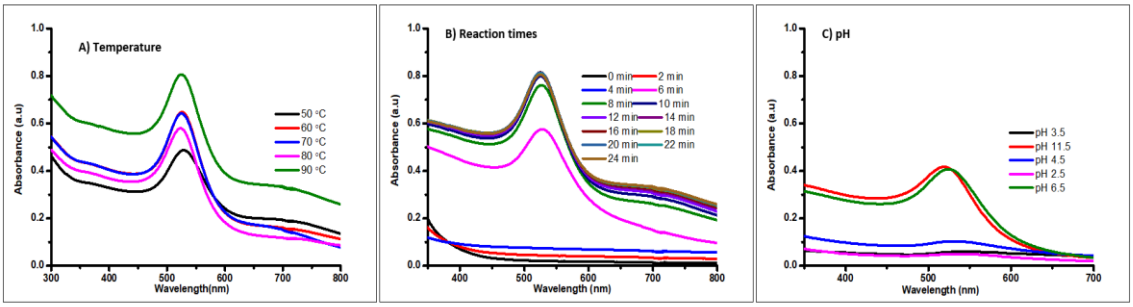

Fig. 1. Absorption spectra of AuNPs synthesized at A) varying temperatures B) varying reaction times C) varying pH of reaction media

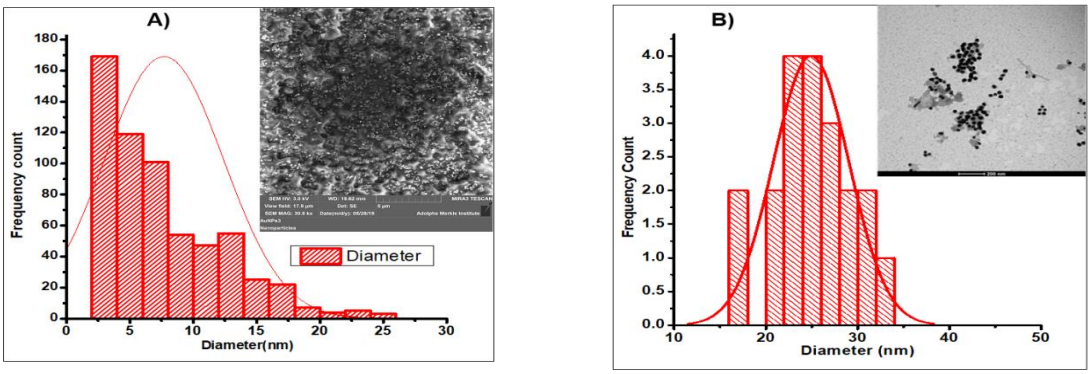

Fig. 2. Size distribution of gold nanoparticles determined by A) Diameter as determined by SEM, insert (SEM micrograph) B) Diameter as determined by TEM, insert (TEM micrograph)

The diameters of the synthesized nanoparticles were determined by TEM and found to have values ranging between 15 to 30 nm (Fig. 2B). In a similar study, researchers investigated the influence of different parameters on the size and morphology of AuNPs using citrate reduction (Tyagi, Kushwaha, Kumar, & Aslam, 2016b) where the AuNPs sizes were estimated between 13 to 25 nm. These results indicate that the growth of AuNPs was not homogeneous since the rate of growth was determined by the relation between the diameter of the growing particle to the amount of gold added.

Hydrodynamic diameter of AuNPs

The results showed that the average hydrodynamic diameters of synthesized particles were in the range of 30-40 nm (Fig. 3).

It was also observed that temperature variation played a role in the synthesized nanoparticles' size, which agrees with observations made under the UV-vis analysis (Fig. 1A). The polydispersibility index and the zeta potential of AuNPs synthesized at the optimum temperature range of 50-90 °C was found to be $5.97e^{-0.001} \pm 1.37e^{-0.001}$ and -0.57 ± 0.48 mV, respectively. Their surface charge influences the dispersed nanoparticles' stability; hence, the developed nanoparticles were highly negative in the present study.

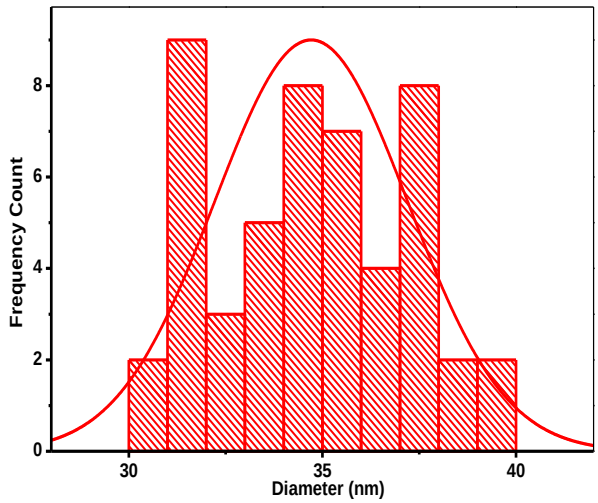

Fig. 3. Hydrodynamic diameters of gold nanoparticles determined by dynamic light scattering

UV-vis spectroscopy

The absorption band of the synthesized colloidal solution in the UV–vis spectrum was centered at 520 nm, which is characteristic of AuNPs. Our result is in agreement with studies conducted by Godoy-reyes and Costero, (2019) and Raj et al. (2015).

When a laser beam was shone through a transparent glass bottle containing the colloidal solution, the presence of individual particles that are large enough to scatter and reflect light in the direction of the observer's eye made the beam visible, as shown in Fig. 4 insert. Such an observation does not occur in true solutions. It indicates the presence of AuNPs in a solution capable of absorbing light within the plasmonic frequency range(Jongjinakool et al., 2014). In the presence of GA solution, a change in colour from brick red to purple was observed after 20 minutes, and the corresponding Uv-vis spectrum showed a shift in SPR band from 520 nm to 700 nm (Fig. 5), an indication of aggregation of AuNPs induced by GA (Klimov and Lambrecht, 2009)

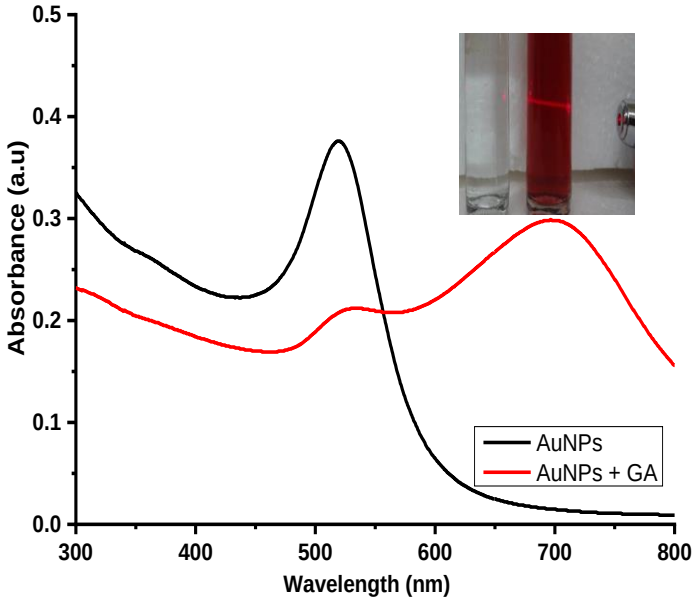

Fig. 4. Absorption spectra of gold nanoparticles (AuNPs) dispersed in aqueous solution before and after the addition of Gibberellic Acid. Insert: Tyndall scattering effect under a 632.8 nm laser beam

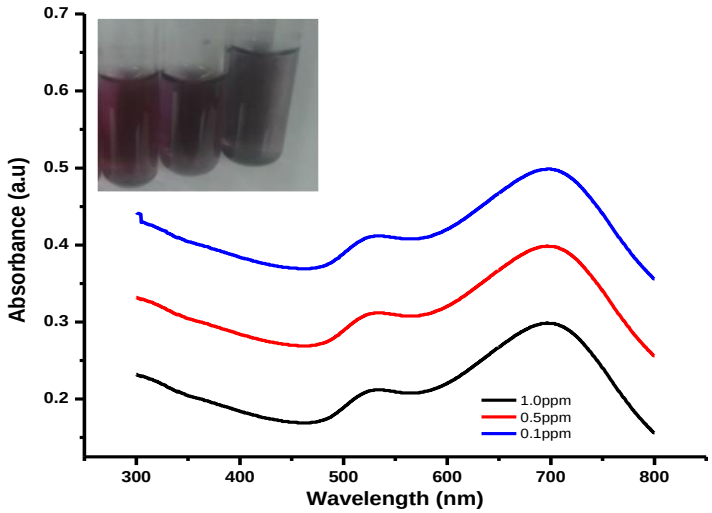

Fig. 5. UV–vis spectra obtained from adding the GA at 0.1 ppm, 0.5 ppm, 1.0 ppm into gold nanoparticles (AuNPs) solution. Insert: Visual colour change

Previous studies conducted by Godoy-reyes and Costero, (2019) indicate the aggregation of cysteine gold nanoparticles (CAuNPs) in the presence of *Escherichia coli* bacteria in urinary tract infection (UTI) patients caused the broadening of spectra and a red-shift.

Quantification of GA_3 from R. solanacearum isolated from soil samples using HPLC

Significantly ($p \leq 0.05$) varying concentrations of GA_3 (83.487 g, 42.543 g, and 31.672 g) were obtained from 10^8, $10^{6,}$ and 10^4 CFU/m L of *R. solanacearum* inoculum, respectively (Table 1).

Real sample analysis

The FT-IR spectra for GA_3 from *R. solanacearum* in comparison with standard GA3 are illustrated in Figure 6. The main characteristic peaks in (Fig. 6) spectra, extracted GA_3 from the local isolate of *R. solanacearum* are at 3449 cm^{-1}, 2985 $cm^{-1,}$ and 1720 cm^{-1}. The peak at 3449 cm^{-1} is attributed to the O-H of the H bond. The peak at 2985 cm^{-1} is attributed to the CH_2 group. The peak at 1720 cm^{-1} can be attributed to the C–O of carboxylic acid. In the IR spectra (Fig. 6), there was no observable difference in the main characteristic absorption bands of standard gibberellic acid and GA_3 extracted from a local isolate of *R. solanacearum* infected soils.

The proposed method was used to detect GA_3 in soil samples from different counties in Kenya. Detection of the presence of *R. solanacearum* using AuNPs was evaluated using UV-vis spectroscopy, and the results are depicted in Fig. 7. Extracted GAs were added to the Red AuNPs solution. The colour changed dramatically from red to purple to blue, confirming the bacterial wilt pathogen in the infected soils.

Table 1*. Peak Height and Peak areas of gibberellic acid (GA_3) extracted from *R. solanacearum* isolates as determined by HPLC

***Ralstonia* concentration (CFU/ml)**	**% Area**	**Retention time**	**Peak height**	**GA_3 concentration (µg/100g)**
$1x10^4$	0.51	6.257	3873	31.672 a
$1x10^6$	0.6	6.297	4927	42.543 a
$1x10^8$	1.3	6.261	10913	83.487 b

* Values within columns followed by the same letter are not significantly different at the 0.05 level of probability.

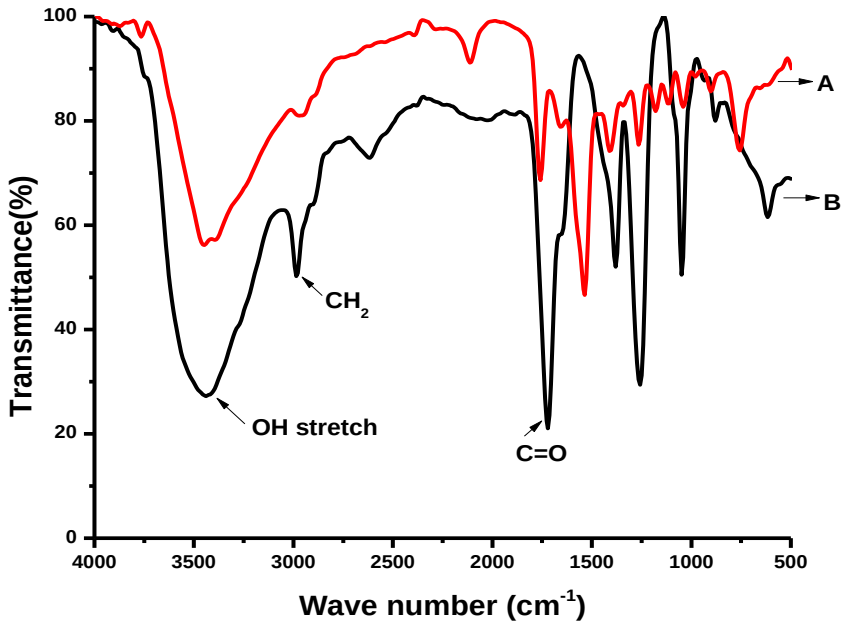

Fig. 6. FT-IR Spectra of gibberellic acid (A): Standard gibberellic acid (GA_3), (B): Extracted gibberellic acid from a local isolate of *R. Solanacearum*

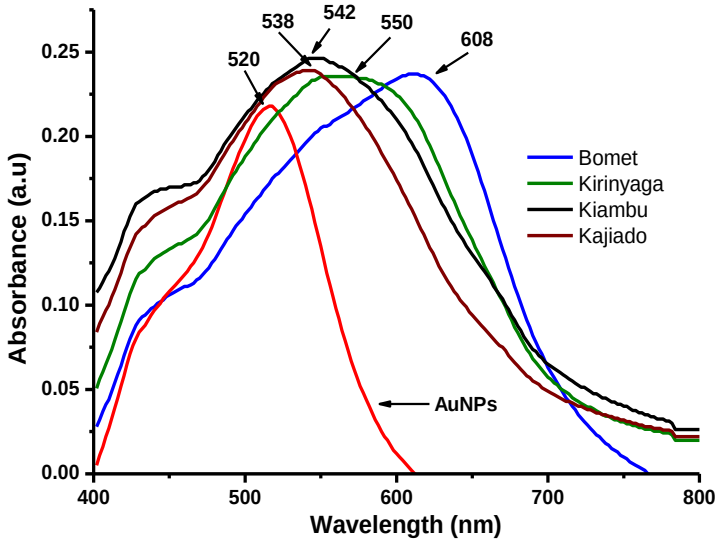

Fig. 7. UV–vis spectra obtained from adding bacterial wilt infected soils into gold nanoparticles (AuNPs) solution

Discussion

As the reaction media temperature increased from 50 to 90 ˚C (Fig. 1A), a hypsochromic shift was observed in the nanoparticles' UV spectra. Changes in surface plasmon resonance (SPR) peaks were also observed with varying reaction times. SPR peaks increased with increasing reaction time until a maximum peak was attained (Fig. 1B). There were no changes in absorbance spectra observed when the reaction media's pH was adjusted to pH 2.5 and 3.5 (Fig. 1C), as demonstrated by the absence of SPR peaks. The absence of the SPR peaks implies that the synthesis of AuNPs did not occur at these particular pH values. However, SPR peaks were observed when the pH was adjusted to pH 6.5 and 11.5 indicating that the synthesis of AuNPs was most appropriate at the two pH values, although a slight bathochromic shift was observed when the pH was at 4.5. A

characteristic wine red color and an absorption band centered at 520 nm further confirm AuNPs synthesis's presence at pH values 6.5 and 11.5. At the macroscale, the element of gold is gold-colored. However, at the nanoscale, the gold element is purple to red, resulting from the scattering of a light beam upon interacting with particles in a colloidal solution. Therefore, the formation of AuNPs can be observed by a change in color. The dispersed nature of the developed nanoparticles was confirmed by both SEM and TEM. It is assumed that an adsorbing layer of citrate anions on the nanoparticles kept the nanoparticles separated. The particles were monodispersed and spherical (Fig. 2 B), which indicated a successful stabilization by adding the citrate ion. This monodispersity is essential for probe preparation in solution and the successful generation of colour signals. The agglomeration of AuNPs induced by varying GA (Sigma-Aldrich) concentration is illustrated in Figure 5. A shift in the SPR band to a longer wavelength of 700 nm (Fig. 5) with a concomitant change in colour to purple was observed. In a study of gold ion reduction by citrate ions, it was reported that citrate functions not only as a reducing agent but also as a stabilizer that prevents the nanoparticles from aggregating (Lin et al., 2011). In solution, AuNPs were stabilized by adsorbed negative ions whose repulsion prevents the strong van der Waals attraction between gold particles from causing them to aggregate (Wang et al., 2015). In GA's presence, an increase in the nanoparticles' size leads to an increase in the scattering of radiation as larger particles scatter more light compared to smaller particles. The probe showed purple color in the presence of GA that was detectable by the naked eye up to a concentration of 0.2 ppm. Increasing GA_3 concentration was observed with increasing inoculum strength with a concentration of 10^8 CFU/mL (the level known to cause bacterial wilt) being significantly different from 10^4 and 10^6 CFU/mL inoculum levels. In similar studies, isolates of fluorescent *Pseudomonas* sp. with GA production ranging from 419-485.8 µg/mL culture were extracted and partially purified. GAs from 28 strains of *Fusarium* were quantified and classified as low, moderate, and high producing (Hamayun et al., 2010; Jiang et al., 2017). These results further corroborate our study finding.In summary, a simplified approach to the standard Turkevich synthesis has been used to develop a colorimetric probe using well dispersed AuNPs for the detection of GA-mediated *R.solanacearum*.

Conclusion

A method to detect and determine the presence of *R. solanacearum* was achieved with the naked eye. The method offers advantages of simplicity, high sensitivity, and convenience. This method relies on the aggregation of AuNPs, which was induced by GA3, causing a colour change from red to purple. The colorimetric sensor shows a red-shift with broadening of the spectrum in the presence of GA-mediated *R. solanacearum*. The high sensitivity AuNPs play a crucial role in designing a pathogen probe with smart sensing properties for field use. The probe will particularly be useful for the pre- and early detection of *R. solanacearum* pathogen. Our study's findings will help farmers identify endemic and non-endemic areas before pathogen establishment and therefore avoid establishing pathogens in such areas, thereby improving tomato production under protected environment and field conditions. The probe can be hosted in nanofibers, thus enhancing shelf-life, portability, and handling.

Acknowledgments

We gratefully acknowledge Mr. Edwin Madivoli for his technical assistance in SEM and TEM analysis.

Funding

This work was supported by Africa-ai-Japan under FY 2018/2019.

Conflict of interests

Authors have declared that no competing interests exist.

Author contributions

Lynn Aoko conducted the experiments, collected and analyzed the data, and wrote the manuscript (original draft preparation and editing). Agnes Kavoo, Dezzline Ondigo, Cornelius Wainaina, and Leonard Kiirika conceptualized the study, provided the resources, supervised, and wrote the manuscript (review and editing). All authors have approved the final article.

References

1. Afroz A, Zahur M, Zeeshan N, Komatsu S. 2013. Plant-bacterium interactions analyzed by proteomics. Frontiers in Plant Science, 4, 1–18.
2. Bertolini E, Olmos A. 2004. Innovative tools for detection of plant pathogenic viruses and bacteria. International Microbology, 6, 233–243.
3. Bhalla K, Singh S.B, Agarwal R. 2010. Quantitative determination of gibberellins by high performance liquid chromatography from various gibberellins producing Fusarium strains. Environmental Monitoring and Assessment, 167(1–4), 515–520.
4. Bottini R, Cassán F, Piccoli P. 2004. Gibberellin production by bacteria and its involvement in plant growth promotion and yield increase. Applied Microbiology and Biotechnology, *65*(5), 497–503.
5. Draz M.S, & Shafiee H. 2018. Applications of gold nanoparticles in virus detection. Theranostics, 8(7), 1985–2017.
6. Godoy-reyes T.M, Costero A.M. 2019. Analytica Chimica Acta Colorimetric detection of normetanephrine, a pheochromocytoma biomarker, using bifunctionalised gold nanoparticles. Analytica Chimica Acta, *1056*, 146–152.
7. Hamayun M, Khan S.A, Khan A.L, Rehman G, Kim Y.H, Iqbal I, Lee I.J. 2010. Gibberellin production and plant growth promotion from pure cultures of *Cladosporium* sp. MH-6 isolated from cucumber (*Cucumis sativus* L.). Mycologia, 102(5), 989–995.
8. Hennessy J, Wilson J. K, Stead D. E, Hutton S, Directive H. 1996. solanacearum in potato tuber extracts. EPPO Bull, 678, 663–678.
9. Huang S, Wang L, Liu L. 2015. Nanotechnology in agriculture , livestock , and aquaculture in China . A review. Agronomy for Sustainable Development, 2015, (28), 369–400.
10. Jazayeri, M. H., Aghaie, T., Avan, A., Vatankhah, A., & Ghaffari, M. R. S. 2018. Colorimetric detection based on gold nano particles (GNPs): An easy, fast, inexpensive, low-cost and short time method in detection of analytes (protein, DNA, and ion). Sensing and Bio-Sensing Research. Elsevier B.V.
11. Jiang G, Wei Z, Xu J, Chen H, Zhang Y, She X. 2017. Bacterial Wilt in China : History , Current Status , and Future Perspectives. Frontiers in Plant Science *8*, 8(September), 1–10.
12. Jing H, Sinha S, Sachar H. S, Das S. 2019. Interactions of gold and silica nanoparticles with plasma membranes get distinguished by the van der Waals forces: Implications for drug delivery, imaging, and theranostics. Colloids and Surfaces B: Biointerfaces, 177(February), 433–439.
13. Jongjinakool S, Palasak K, Bousod N, Teepoo S. 2014. Gold nanoparticles-based colorimetric sensor for cysteine detection. Energy Procedia, 56(C), 10–18.
14. Kapoor, R., Soni, R., & Kaur, M. 2016. Gibberellins production by fluorescent Pseudomonas isolated from Rhizospheric soil of Malus and Pyrus. International Journal of Agriculture, Environment and Biotechnology, *9*(April), 193–199.
15. Karuku G. N, Kimenju J.W, Verplancke H. 2017. Farmers' perspectives on factors limiting tomato production and yields in Kabete, Kiambu County, Kenya. East African Agricultural and Forestry Journal, *82*(1), 70–89.
16. Katznelson H, Cole S.E. 1965. Production of Gibberellin-Like Substances By Bacteria and Actinomycetes. Canadian Journal of Microbiology, *11*(4), 733–741.
17. Khan A. 2014. Gold nanoparticles : Synthesis and applications in drug delivery Gold Nanoparticles : Synthesis and Applications in Drug. Synthesis and Applications in Drug, (July).

18. Kim S.H, Oh S.S, Kim K.J, Kim J.E, Park H.Y, Hess O, Kee C.S. 2015. Subwavelength localization and toroidal dipole moment of spoof surface plasmon polaritons. Physical Review B - Condensed Matter and Materials Physics, *91*(3), 1–9.

19. Klimov V.V, Lambrecht A. 2009. Van der waals forces between plasmonic nanoparticles. Plasmonics, 4(1), 31–36.

20. Li D Wieckowska A Willner I. 2008. Optical Analysis of Hg^{2+} Ions by Oligonucleotide – Gold-Nanoparticle Hybrids and DNA-Based Machines, *Angewandte Chemie*, *120*, 3991–3995.

21. Lin Y.W, Huang, C.C, Chang H.T. 2011. Gold nanoparticle probes for the detection of mercury, lead and copper ions. Analyst.

22. Madivoli, E.S, Kareru P.G, Gachanja A.N, Mugo S. M, Sujee D.M, Fromm K.M. 2020. Isolation of Cellulose Nanofibers from Oryza sativa Residues via TEMPO Mediated Oxidation. Journal of Natural Fibers, *5*, 1–13.

23. Mansfield J, Genin S, Magori S, Citovsky V, Sriariyanum M, Ronald P, Tolosan F.C. 2012. Top 10 plant pathogenic bacteria in molecular plant pathology. Molecular Plant Pathology. *13*, *13*, 614–629.

24. Mirkin C.A, Letsinger R.L, Mucic R.C, Storhoff J.J. 1996. A DNA-based method for rationally assembling nanoparticles into macroscopic materials. Nature, 382(6592), 607–609.

25. Murigi M.K, Madivoli E.S, Mathenyu M.M, Kareru P.G, Gachanja A.N, Njenga P.K, Githua M. 2014. Comparison of Physicochemical Characteristics of Microcrystalline Cellulose from Four Abundant Kenyan Biomasses. IOSR Journal of Polymer and Textile Engineering, 1(2), 53–63.

26. Ngumbi P.K, Mugo S.W, Ngaruiya J.M. 2018. Determination of Gold Nanoparticles Sizes via Surface Plasmon Resonance. IOSR Journal of Applied Chemistry (IOSR-JAC, 11(7), 25–29.

27. Park J, Shumaker-parry J.S. 2020. Structural Study of Citrate Layers on Gold Nanoparticles: Role of Intermolecular Interactions in Stabilizing Nanoparticles. Journal of the American Chemical Society, 136, 1907–1921.

28. Ponce C, Chanona J, Garibay V, Palacios E, Calderon G, Sabo R. 2013. Functionalization of Agave Cellulose Nanoparticles and its Characterization by Microscopy and Spectroscopy Techniques. Microscopy and Microanalysis, 19(S2), 200–201.

29. Primo E.D, Ruiz F, Masciarelli O, Giordano W. 2015. Bacterial Metabolites in Sustainable Agroecosystem. In Bacterial Metabolites in Sustainable Agroecosystem (Vol. 12, pp. 337–349).

30. Raj V, Vijayan A.N, Joseph K. 2015. Cysteine capped gold nanoparticles for naked eye detection of E. coli bacteria in UTI patients. Sensing and Bio-Sensing Research, *5*, 33–36.

31. Sarkar S, Chaudhuri S. 2016. Bacterial wilt and its management. Current Science, 110(8), 1439–1445.

32. Sciences P, Sabir S, Asghar H.N, Kashif S.U.R, Khan M.Y, Akhtar M.J, Sciences A. 2013. Synergistic effect of plant growth promoting rhizobacteria and kinetin on maize. Journal of Animal and Plant Sciences.23(6), 1750–1755.

33. Selvarajan R, Selvam K.P, Balasubramanian V, Sundaram S.S. 2020. A rapid and sensitive lateral flow immunoassay (LFIA) test for the on-site detection of banana bract mosaic virus in banana plants. Journal of Virological Methods, (May), 113929.

34. Sharma S, Sharma A, Kaur M. 2018. Extraction and evaluation of gibberellic acid from Pseudomonas sp .: Plant growth promoting rhizobacteria. Journal of Pharmacognosy and Phytochemistry, *7*(1), 2790–2795.

35. Slistan-Grijalva A, Herrera-Urbina R, Rivas-Silva J.F, Ávalos-Borja M, Castillón-Barraza F.F, Posada-Amarillas A. 2005. Classical theoretical characterization of the surface plasmon absorption band for silver spherical nanoparticles suspended in water and ethylene glycol. Physica E: Low-Dimensional Systems and Nanostructures, 27(1–2), 104–112.

36. Stevens K.A, Jaykus L. 2014. Bacterial Separation and Concentration from Complex Sample Matrices : A Bacterial Separation and Concentration from Complex Sample Matrices : A Review. Critical Reviews in Microbiology. 30, 30(February), 7–24.

37. Tyagi H, Kushwaha A, Kumar A, Aslam M. 2016a. A Facile pH Controlled Citrate-Based Reduction Method for Gold Nanoparticle Synthesis at Room Temperature. Nanoscale Research Letters, (August).

38. Tyagi H, Kushwaha A, Kumar A, Aslam M. 2016b. A Facile pH Controlled Citrate-Based Reduction Method for Gold Nanoparticle Synthesis at Room Temperature. Nanoscale Research Letters, 11(1), 362.

39. Verma, H. N., Singh, P., & Chavan, R. M. 2014. Gold nanoparticle: Synthesis and characterization. Veterinary World, 7(2), 72–77.

40. Wang Z, Fang C, Mallavarapu M. 2015. Characterization of iron – polyphenol complex nanoparticles synthesized by Sage (Salvia officinalis) leaves Environmental Technology & Innovation4, (May), 92–97.